

Excited-state spectroscopy of InP quantum dots

D. Bertram, O. I. Mičić, and A. J. Nozik

National Renewable Energy Laboratory, 1617 Cole Boulevard, Golden, Colorado 80401

(Received 14 October 1997)

We have measured low-temperature size-selective photoluminescence excitation spectra of high-quality InP quantum dots prepared by colloidal chemistry. A set of samples with mean emission energies in the range from 1.9 to 2.2 eV was investigated. All samples have a size distribution of about 10%, resulting in an inhomogeneously broadened photoluminescence lineshape. Due to the finite size distribution, spectra were collected at different detection wavelengths to reveal the energies of the excited excitonic states. The size dependence of the quantization energies of InP nanoparticles was determined by measuring photoluminescence excitation at different detection energies within one sample. Up to eight excited-state transitions in a set of seven samples were observed, as the estimated quantum dot size was scanned from 1.8 to 4.0 nm. A comparison of the observed peaks with a six-band $\mathbf{k}\cdot\mathbf{p}$ calculation is given. In contrast to the successful interpretation in the case of CdSe, no agreement between the calculated and the observed excited-state energies is achieved. [S0163-1829(98)50708-4]

Quantum dots (QD's) continue to receive great attention because of the three-dimensional confinement of their electronic particles; they attract a very high level of activity because of their interesting basic physics and potential applications.¹ Two main approaches for fabricating these small quantized structures have emerged: (1) epitaxial growth of QD's in various material systems²⁻⁷ in the Stranski-Krastanov growth mode that typically forms pyramidal QD islands that are usually 10–15 nm in base width and 5 nm in height, and (2) QD's derived by colloidal chemistry, producing very small-sized, nearly spherical nanocrystalline particles ranging in diameter from about 1 to 10 nm.⁸⁻¹⁰ Both methods, however, have to cope with a significant distribution of the QD size and thus with a distribution of the energy levels of the QD states in ensemble measurements.

Comparing the size of the QD's with the Bohr radius of the bulk exciton, the first class of quantum dots is usually in the weak confinement regime, where only a small number of bound states is observable and where the QD's are also usually coupled via the wetting layer. The colloidal nanoparticles, on the other hand, can be in the strong confinement regime when the particle size is small (<5 nm); the wave functions of electrons and holes are localized in the zero-dimensional structure, and because of the high potential barrier with the surrounding matrix, they manifest additional higher excited states for both electrons and holes. Although much investigation has been conducted in order to reveal the basic physical properties of colloidal QD's, most of the work on these types of nanostructures has been done on the II-VI material system because of the ease of preparation of high-quality samples.¹¹⁻¹⁸

In this paper we report on low-temperature photoluminescence excitation (PLE) measurements on InP nanocrystallites which were derived from wet chemical preparation. Details of the chemistry are published elsewhere.^{10,19} The good quality of the prepared quantum dot samples and the comparably narrow size distribution has already been demonstrated.²⁰ To obtain further insight into the size dependence of the elec-

tronic structure, we performed size-selective low-temperature PLE measurements. This technique reveals the excited state transitions by optically selecting an ensemble of specific-sized QD's.²¹

A set of samples is investigated having mean peak PL emission energies that span a range between 1.9 and 2.4 eV, which corresponds to a mean size range between 2.4 and 3.4 nm, respectively. The size of the quantum dots and the main emission energy is related via²²

$$E_g(d) = E_g^{\text{bulk}} + \frac{A}{d^n}, \quad (1)$$

where $E_g^{\text{bulk}} = 1.45$ eV is the low-temperature band gap of bulk InP, $A = 55.2527$ and $n = 1.3611$.

The present measurements were carried out using a SPEX Fluorolog 2 spectrophotometer. Excitation was provided from a Xe-arc lamp. The emission from the lamp was dispersed in a 0.22 m double monochromator and focused onto the sample. The sample was mounted in an Oxford CFV 1204 continuous flow cryostat, where the sample was cooled by He vapor as exchange gas.

All samples are colloidal solutions of InP nanoparticles capped with oleyamine and dissolved in 2,2,4 trimethylpentane which contains 2–5% oleyamine; these solutions form an optically clear organic glass at cryogenic temperatures. The concentration of the InP QD's was adjusted to provide optical densities of 0.1 at 450 nm in matched 1 mm quartz cuvettes in order to prevent energy transfer between different sized QD's within a sample. This phenomenon, which has been shown to occur in close-packed structures of InP QD's,²³ is reduced due to the reduced volume density of the particles and the increased separation between the QD's. Therefore, we are able to measure different sized QD's by just changing the detection wavelength within one sample. The emission of the samples is dispersed in a second 0.22 m double monochromator and subsequently focused onto a photomultiplier tube (PMT). The resulting spectra are nor-

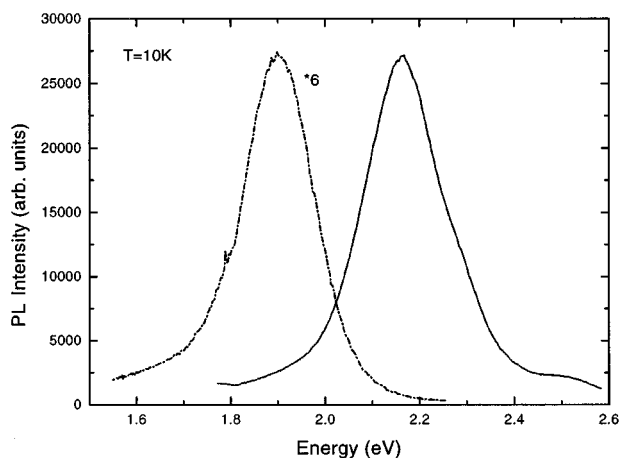


FIG. 1. Low-temperature PL spectra of the smallest and the largest sized QD samples investigated.

malized to a simultaneously recorded reference file, correcting for the spectral variation of the excitation density. All spectra are taken at 10 K.

Typical PL spectra of the smallest and largest sized QD samples, excited at 2.76 eV, are shown in Fig. 1. As can be seen from the plot, both emission lines are inhomogeneously broadened, indicating a significant size distribution within the samples. The intensities, as well as the full width at half maximum (FWHM), are of comparable magnitude for all samples, and show the reproducibility of the synthesis of the InP QD's. The emission is shifted to higher energies compared with bulk InP, due to size quantization effects. The range of emission energies from all investigated samples extends from 1.6 to 2.55 eV.

To investigate the size dependence of the excited excitonic states we performed low-temperature PLE measurements at different detection wavelengths on the high-energy side of the emission range of each of the samples. Since every sample has an inherent distribution of sizes, a variation of the detection wavelength selects different sized quantum dots within one sample, thus allowing for a measurement of the size dependence of the subband structure in the strong zero-dimensional confinement regime.

A set of PLE spectra obtained for a sample with mean QD diameter of 3.0 nm is shown as an example, together with the respective emission peak, in Fig. 2. The detection wavelengths of the first and last PLE spectrum are indicated by arrows in the PL spectrum. As can be seen from this figure we obtain several peaks in the PLE trace indicating absorption by excited states and subsequent emission after relaxation into the ground state. With increasing detection energy, i.e., decreasing size of the QD's under investigation, these peaks also shift to higher energies, indicating an increase in size quantization energy. Although the detected luminescence bandwidth is small at a certain wavelength, the measured peaks in the PLE spectra are still inhomogeneously broadened. A small peak at 2.9 eV which does not shift with detection energy was found to be an artifact of the excitation source and is ignored in the analysis of the PLE spectra.

By measuring seven different samples in which the emission energies ranged from 1.6 to 2.55 eV, a broad range of different sized quantum dots is sampled to determine the size dependence of the excited-state energy-level structure of the

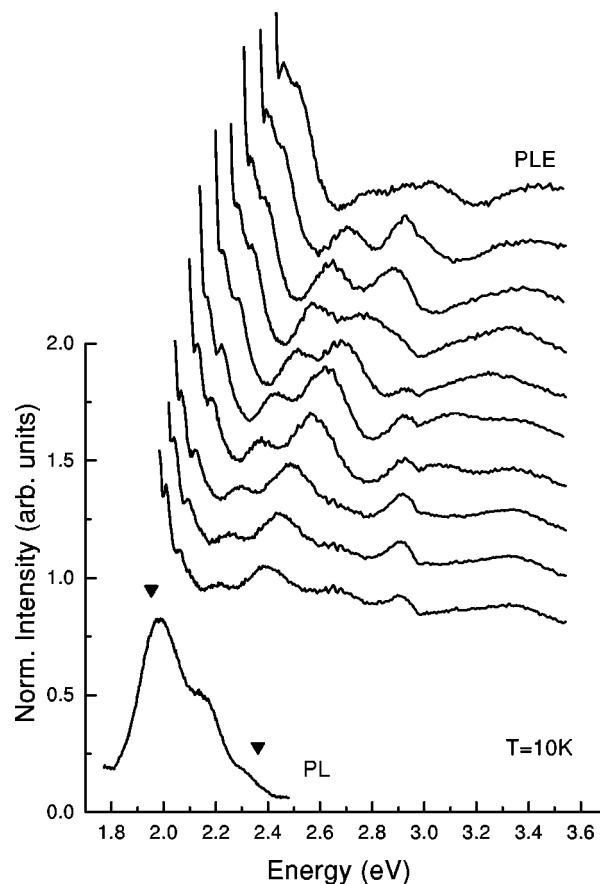


FIG. 2. Series of PLE spectra taken for one sample at different detection wavelengths. The interval where PLE spectra are taken is indicated by arrows on the PL curve.

nanoparticles. In this way a continuous ensemble of QD's with diameters from 1.8 to 4.0 nm is investigated.

The peaks in the PLE spectra were fitted to a Gaussian lineshape to evaluate the peak energy and to separate the contributions from different maxima. The result of the procedure is shown, for all recorded PLE spectra, in Fig. 3. Here the difference, ΔE , between the energy of the peak in the PLE spectrum and the detection energy is plotted as a function of the bandgap. Since the emission, and therefore the detection energy, is essentially a measure of the bandgap and thus the size of the quantum dot, the x coordinate can also be interpreted via the bandgap energy as a size scale of the nanoparticles. On the other hand, the y scale is a measure of the energy separation of the excited-state transitions in the quantum dots. The upper part of the plot shows all observed transitions, whereas the lower part of Fig. 3 reproduces the results for small ΔE on a magnified scale.

As can be seen from the plot, several lines corresponding to excited-state transitions can be resolved, shifting to higher energies with increasing bandgap (i.e., detection) energy. The majority of the peaks are shifting with different slopes and several crossings and anticrossings are suggested by the data (as, e.g., around 2.1 eV in the upper part of Fig. 3). Up to eight excited-state transitions are apparent from analyzing the seven samples, although a single sample usually showed up to six transitions. The lower part of Fig. 3 reproduces the first three transitions measured in the PLE spectra. The horizontal bold line indicates the longitudinal optical (LO) pho-

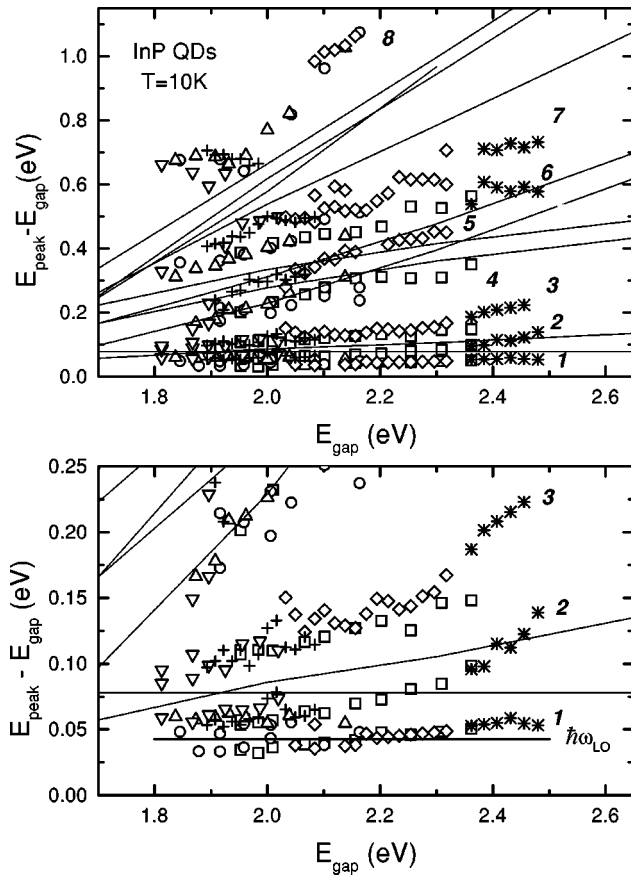


FIG. 3. Difference between peak energy in the PLE spectrum and detection energy for all recorded spectra. The detection energy is assumed to equal the bandgap transition of the specific-sized quantum dots within the investigated sample. The lower part reproduces the lowest energy transitions of the upper plot on an enlarged scale. Data are represented by symbols, theoretical results based on a standard six-band $\mathbf{k}\cdot\mathbf{p}$ calculation are shown as thin lines. The bold line denotes the bulk LO-phonon energy of InP.

non energy in bulk InP. It can be seen from the figure that a LO-phonon-assisted absorption with a constant phonon energy of $\hbar\omega_{\text{LO,InP}}^{\text{bulk}}$ is not entirely consistent with our data. As can be seen from Fig. 3, the lowest energy transition (labeled 1) increases slightly with increasing energy gap. It is possible that the LO-phonon energy increases moderately with decreasing size of the QD's, which would make the first transition in Fig. 3 consistent with LO-phonon-assisted absorption.

To assign the different transitions observed, we compare the measured data with the results of a six-band $\mathbf{k}\cdot\mathbf{p}$ calculation²⁴ of the single-particle bound electron and hole states, and the resulting expected transition energies (cf. Fig. 3). This model has been applied to CdSe and InP QD's by Norris and Bawendi,^{11,12} and Banin *et al.*,²⁵ respectively. Their calculations, using a 6×6 $\mathbf{k}\cdot\mathbf{p}$ model with nonparabolicity corrections to the conduction band represents the states of the QD's in terms of the states of the periodic bulk solid at the $k=0$ Brillouin zone center. We have extended this method, that successfully accounted for up to ten excited states in CdSe^{11,12} to InP. We use the Vahala and Sercel approach²⁶ as implemented numerically by Fu and Zunger.²⁴ The (isotropic) Luttinger parameters are taken from experi-

mental data on bulk InP (Ref. 27) as $\gamma_1=6.28$ and $\gamma=(2\gamma_2+3\gamma_3)/5=2.49$. We assume the same electron-hole Coulomb energies for all excited states. This calculation produces nearly identical results as those of Banin *et al.*²⁵ The two lowest transitions $1p_{3/2}-1s_e$ and $1p_{1/2}-1s_e$ are dipole forbidden, whereas the lowest allowed transitions in increasing order of energy are $1s_{3/2}-1s_e$, $1s_{1/2}-1s_e$, and $2s_{3/2}-1s_e$. These calculated allowed transitions do not fit the experimental data (cf. Fig. 3) and we find a qualitative difference between the slope of the plot of observed differences in transition energies vs. bandgap and the 6×6 $\mathbf{k}\cdot\mathbf{p}$ calculations: while the model predicts that the three lowest energy allowed transitions have a near constant energy shift relative to the bandgap, the measurements (e.g., lines 2,3 in Fig. 3) show a superlinear upward bend of the slope of the measured transitions with decreasing size. Even if we take into account forbidden transitions from p -like valence-band states to s -like conduction-band states, the standard^{11,12} $\mathbf{k}\cdot\mathbf{p}$ calculation still does not match the experimental data. However, it has to be noted here that no LO-phonon-assisted transitions are included in the calculations, which may have a significant contribution to the data.

In a second approach for calculating the level structure, the effective masses used in the $\mathbf{k}\cdot\mathbf{p}$ calculations were adjusted to fit the more rigorous pseudopotential results.²² The fit was poor (yielding $\gamma_1=1.59$; $\gamma=0.34$), but it did succeed in changing the order of the QD highest valence-band states such that the $1s_{3/2}$ level is above the $1p_{3/2}$ level as obtained by pseudopotential calculations.²² However, even with the somehow arbitrary method described above, we could not match the experimental data if only the dipole allowed transitions were taken into consideration. On the other hand, if all possible allowed and nonallowed transitions between electron and hole levels are considered (see below), we are able to qualitatively assign the observed peaks in the PLE spectra. This leads us to assign the 0 eV line to the bandgap transition $1s_{3/2}-1s_e$ of the QD's. This is in contradiction to other recent $\mathbf{k}\cdot\mathbf{p}$ calculations that predict the 0 eV line should be $1p_{3/2}-1p_e$.^{25,28}

The first peak in PLE should be the resonant redshift^{22,29} resulting from the splitting of the lowest conduction band state by electron-hole exchange. These values have previously been measured²⁹ and analyzed.^{22,29} This transition, which has a very small energy splitting (6–20 meV) is not observed in our spectra because it is outside the resolution of the present experiment. On the basis of the adjusted $\mathbf{k}\cdot\mathbf{p}$ calculation, we assign the second transition appearing in PLE (2 in Fig. 3) to the dipole forbidden excitation from the first excited valence-band state to the lowest conduction band state ($1p_{3/2}-1s_e$). This follows because in the 6×6 $\mathbf{k}\cdot\mathbf{p}$ model the conduction band quantization energies are of the order of several hundred meV in the investigated size regime.²⁴ The next higher transition, labeled 3 in the plot, corresponds approximately to the dipole forbidden transition between the $1p_{1/2}-1s_e$ states. Transition 4 in the upper part of Fig. 3, is qualitatively reproduced by the calculated $2s_{3/2}-1s_e$. However, surprisingly no transition was found corresponding to the $1s_{1/2}-1s_e$ energy. We assign the experimental transitions 5–7 to higher valence-band states since PLE peaks involving the first excited conduction-band state can correspond energetically only to the highest observed transi-

tion (labeled 8 in Fig. 3). A more detailed and rigorous analysis of the energy-level structure of InP QD's using an exact pseudopotential method is under way;²⁴ this will permit a more strict and detailed comparison of the experimental data with theoretical energy-level calculations.

Another feature observed in our PLE spectra is an anticrossing and crossing of transitions within the range of measured QD's. This can be seen, e.g., in the region around 2.15 eV for the excited-state transitions as well as around 1.95 eV for the highest transition. It is expected from the calculations^{11,12} that the differences in size dependence of the quantization energy of the different valence-band states will account for the crossings suggested by the experimental data.

In conclusion, we have measured the size dependence of the excited-state transitions of InP QD's in the strong confinement regime. By using size-selective spectroscopy techniques, we were able to scan a QD size range from 1.8 to 4.0 nm, and determine higher transitions within the absorption

spectra of the QD's. A rich structure was found which is inconsistent with conventional $\mathbf{k}\cdot\mathbf{p}$ calculations, using either bulk-measured or empirically adjusted effective masses and considering only dipole allowed transitions as well as assuming equal Coulomb interaction for all excited states. However, taking into account dipole forbidden transitions, a qualitative agreement with the adjusted effective mass $\mathbf{k}\cdot\mathbf{p}$ calculation leads to an assignment of the observed transitions. A detailed model representing the full observed energy-level structure as well as level crossings remains to be developed.

This work was supported by the U.S. Department of Energy, Office of Basic Energy Science, Division of Chemical Sciences. Fruitful discussions with A. Zunger, H. Fu, and L. W. Wang are gratefully acknowledged. Thanks are given to H. Fu for performing the $\mathbf{k}\cdot\mathbf{p}$ calculations. D.B. wishes to thank the German research society DFG for support under Grant No. 1999/BE-1.

¹C. Weisbuch and B. Vinter, *Quantum Semiconductor Structures: Fundamentals and Applications* (Academic, New York 1991).

²W. Seifert, N. Carlsson, M. Miller, M. E. Pistol, L. Samuelson, and L. R. Wallenberg, *Prog. Cryst. Growth Charact. Mater.* **33**, 423 (1996).

³M. C. Hanna, Z. H. Lu, A. F. Cahill, M. J. Heben, and A. J. Nozik, *J. Cryst. Growth* **174**, 605 (1997).

⁴A. Mews, A. V. Kadavanich, U. Banin, and A. P. Alivisatos, *Phys. Rev. B* **53**, 13 242 (1996).

⁵A. Kurtenbach, K. Eberl, and T. Shitara, *Appl. Phys. Lett.* **66**, 361 (1995).

⁶M. Grundmann, N. N. Ledentsov, R. Heitz, L. Eeckey, J. Christen, J. Bohrer, D. Bimberg, S. S. Ruvimov, P. Werner, U. Richter, J. Heydenreich, V. M. Ustinov, A. Y. Egorov, A. E. Zhukov, P. S. Kopev, and Z. I. Alferov, *Phys. Status Solidi B* **188**, 249 (1995).

⁷R. Apetz, L. Vescan, A. Hartmann, R. Loo, C. Dieker, R. Carius, and H. Luth, *Mater. Sci. Technol.* **11**, 425 (1995).

⁸C. B. Murray, C. R. Kagan, and M. G. Bawendi, *Science* **270**, 1335 (1995).

⁹A. A. Guzelian, U. Banin, A. V. Kadavanich, X. Peng, and A. P. Alivisatos, *Appl. Phys. Lett.* **69**, 1432 (1996).

¹⁰O. I. Mićić, C. J. Curtis, J. R. Sprague, K. M. Jones, and A. J. Nozik, *J. Phys. Chem.* **98**, 4966 (1994).

¹¹D. J. Norris and M. G. Bawendi, *Phys. Rev. B* **53**, 16 338 (1996).

¹²D. J. Norris and M. G. Bawendi, *J. Chem. Phys.* **103**, 5260 (1995).

¹³P. A. M. Rodrigues, G. Tamulaitis, P. Y. Yu, and S. H. Risbud, *Solid State Commun.* **94**, 583 (1995).

¹⁴S. A. Blanton, R. L. Leheny, M. A. Hines, and P. Guyot-Sionnest, *Phys. Rev. Lett.* **79**, 865 (1997).

¹⁵D. J. Norris, A. L. Efros, M. Rosen, and M. G. Bawendi, *Phys. Rev. B* **53**, 16 347 (1996).

¹⁶U. Banin, J. C. Lee, A. A. Guzelian, and A. P. Alivisatos (unpublished).

¹⁷S. A. Empedocles, D. J. Norris, and M. G. Bawendi, *Phys. Rev. Lett.* **77**, 3873 (1996).

¹⁸A. D. Yoffe, *Adv. Phys.* **42**, 173 (1993).

¹⁹O. I. Mićić, J. R. Sprague, C. J. Curtis, K. M. Jones, J. L. Machol, A. J. Nozik, H. Giessen, B. Fluegel, G. Mohs, and N. Peyghambarian, *J. Phys. Chem.* **99**, 7754 (1995).

²⁰O. I. Mićić, J. Sprague, Z. Lu, and A. J. Nozik, *Appl. Phys. Lett.* **68**, 3150 (1996).

²¹M. G. Bawendi, W. L. Wilson, L. Rothberg, P. J. Carroll, T. M. Jedju, M. L. Steigerwald, and L. E. Brus, *Phys. Rev. Lett.* **65**, 1623 (1990).

²²H. Fu and A. Zunger, *Phys. Rev. B* **55**, 1642 (1997); *Appl. Phys. Lett.* (to be published).

²³O. Mićić, K. Jones, A. Cahill, A. Zaban, and A. J. Nozik (unpublished).

²⁴H. Fu and A. Zunger (private communication).

²⁵U. Banin, C. Gerullo, A. A. Guzelian, C. J. Bardeen, A. P. Alivisatos, and C. V. Shank, *Phys. Rev. B* **55**, 7059 (1997).

²⁶K. J. Vahala and P. C. Sercel, *Phys. Rev. Lett.* **65**, 239 (1990).

²⁷D. Bimburg *et al.*, in *Physics of Group IV Elements and III-V Compounds*, edited by O. Madelung, Landolt-Börnstein, New Series, Group 3, Vol. 17, Pt. a (Springer-Verlag, Berlin, 1982).

²⁸A. L. Efros (private communication).

²⁹O. I. Mićić, H. M. Cheong, H. Fu, A. Zunger, J. R. Sprague, A. Mascarenhas, and A. J. Nozik, *J. Phys. Chem.* **101**, 4904 (1997).